

# Synthesis and Characterization of Novel Modified SBA-15/PSF Nanocomposite Membrane Coated by PDMS for Gas Separation

**A. Jomekian**

e-mail: abolfazl.jomekian@gmail.com

**M. Pakizeh**

e-mail: pakizeh@um.ac.ir

**M. Poorafshari**

e-mail: poorafshari@um.ac.ir

**S. A. A. Mansoori**

e-mail: bidad\_kavir@yahoo.com

Department of Chemical Engineering,  
Faculty of Engineering,  
Ferdowsi University of Mashhad,  
Mashhad 91775-1111, Iran

*SBA-15 nanoparticles were prepared by in situ assembly of inorganic precursors and CTAB. The structure of nanoparticles was characterized by X-ray diffraction, transmission electron microscopy, particle size analysis, and  $N_2$  adsorption techniques. The surface modification of particles in order to perfect dispersion in PSF matrix was performed by DMDCS and APTMS as new modification agents. Thermogravimetric analysis and scanning electron microscopy analysis were applied to investigate thermal stability and quality of distribution of particle in the nanocomposite membrane, respectively. The PDMS was used to coat the possible defects of synthesized membranes. For all gases ( $N_2$ ,  $CO_2$ ,  $CH_4$ , and  $O_2$ ), the permeance of uncoated DMDCS modified SBA-15/PSF (20 wt %) raised from 16 to 31.6, 0.47–0.99, 0.45–1.1 and 2.75–5.33 for  $CO_2$ ,  $N_2$ ,  $CH_4$ , and  $O_2$ , respectively in comparison with PSF. The corresponding values of  $CO_2$ ,  $N_2$ ,  $CH_4$ , and  $O_2$  permeances through uncoated APTMS modified SBA-15/PSF (20 wt %) enhanced to 29.12, 0.8, 0.85, and 4.75 respectively, compared with neat PSF membrane. The ideal selectivities of  $CO_2/CH_4$  and  $O_2/N_2$  for DMDCS modified SBA-15 (20 wt %) nanocomposite membranes coated by 30 wt % PDMS solution enhanced from 26 to 35 and from 5.4 to 7.1, respectively. Using APTMS as modification agent resulted in higher selectivity of  $CO_2/CH_4$  (38.2) and  $O_2/N_2$  (7.2) than those of DMDCS modified. The measured actual selectivities of  $CO_2/CH_4$  and  $O_2/N_2$  and permeances of all gases tested are a few amounts lower than ideal selectivities and permeances of gases in single gas permeation tests but are still much higher than those for pure PSF. [DOI: 10.1115/1.4003862]*

**Keywords:** modified SBA-15, polysulfone, PDMS, nanocomposite membrane

## 1 Introduction

Polymeric membranes have been very useful in addressing industrially important gas separations, thereby providing economical alternatives to conventional separation processes. However, there is always a trade-off between permeability and selectivity of these membranes for gas separation applications as shown in the upper bound curves developed by Robeson [1]. The intrinsic property of polymers limited their use in gas separation processes. Therefore, there is a need for innovation in polymeric membrane technology so that the new types of membranes can successfully be used in these applications [2–5]. An important recent discovery in the membrane science is the polymer nanocomposite membrane [6–9]. Here in this structurally engineered nanocomposite membranes, the nanoparticles act as to create preferential permeation pathways for selective permeation while posing a barrier for undesired permeation in order to improve separation performance [3]. In recent years, significant improvements in the performance of polymer nanocomposite membranes for gas separation have been made. Clearly the success of the polymer nanocomposite membranes depends largely on the quality of the interface between the nanofiller and the polymer [10–13]. Ordered mesoporous silicas (OMSs) are a class of materials possessing unique properties at the nanoscale and can be used as nanofiller in polymer matrix. Since their initial discovery by the Mobil Laboratory

in the early 1990s, these materials have been heavily investigated. These porous solids have desirable properties including highly uniform pore sizes in the 2–10 nm range that possess long-range order, despite that the matrix material is amorphous silica [4,5]. Recently, mesoporous molecular sieves have been used in nanocomposite membranes to enhance permeability or selectivity of polymeric membranes [14,15]. As a remarkable work, an application of polysulfone (PSF) nanocomposite membrane with mesoporous MCM-41 for gas separation has been reported [16]. Kim et al. [17,18] enhanced gas permeability of PSF by incorporating mesoporous MCM-48. They showed that the permeability of PSF nanocomposite membrane increased by introducing mesoporous materials, whereas the selectivity did not change significantly and that was because of suitable compatibility between nanoparticles and polymer matrix. However, in these cases the selectivity performance of membranes has not been improved and this important property of membrane has remained unchanged. The introduction of nanoscale inorganic particles in polymer matrix should give more polymer/particle interfacial area and provide the chance to introduce higher loading of the molecular sieves into the polymer matrix. Additionally, nanoscale molecular sieves are more suitable for commercialization of nanocomposite membranes whereas they have very thin selective layers than micron-sized zeolites or molecular sieves. Recently, the additional functionalization of nanofiller surface in order to enhance the sorption effects of these particles and therefore raise gas selectivity or providing proper adherence between inorganic and organic phases have been considered by researchers [19–21]. In this study, as a

Manuscript received December 20, 2010; final manuscript received March 2, 2011; published online May 13, 2011. Editor: Vijay K. Varadan.

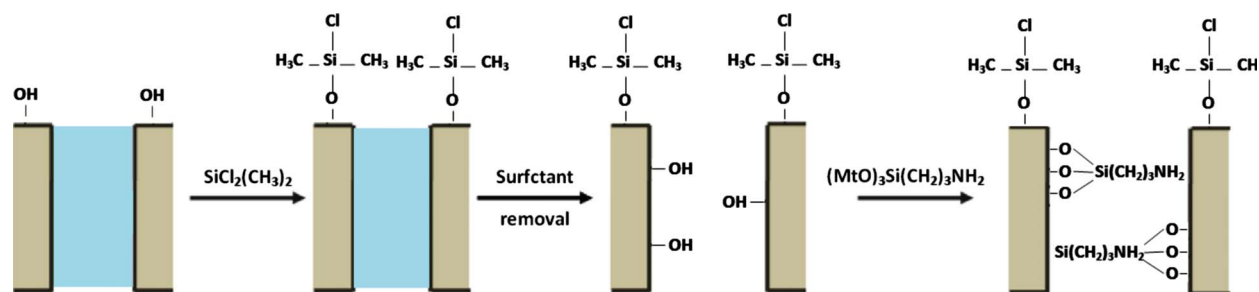


Fig. 1 Silylation and amine treatment of SBA-15 nanoparticles

new work, the functionalization of particles was performed by dimethyldichlorosilane (DMDCS) and aminopropyltrimethoxysilane (APTMS) as new modification agents. Several studies have been carried out on transport properties of pure and binary gas mixtures of  $O_2$ ,  $N_2$ ,  $CO_2$ , and  $CH_4$  using PDMS membrane [22–24]. Hence, as a new approach, we decided to use this high permeable polymer to coat the surface of nanocomposite SBA-15/PSF membrane in order to fill the possible surface voids and improve membrane selectivity for gas separation. The main purpose of this study is the fabrication and characterization of two new modified SBA-15/PSF nanocomposite membranes, which coated by PDMS in order to gain the superior gas separation properties compared with neat polymeric membranes. In the first step, SBA-15 nanoparticles was produced in hydrothermal route, and then its structure was investigated with several adequate characterization methods containing particle size analysis, X-ray diffraction (XRD) analysis, pore size analysis, and transmission electron microscopy (TEM). The effect of inorganic nanofiller on thermal stability nanocomposite membranes was studied by TGA. The scanning electron microscopy (SEM) was used to investigate the quality of modified obtained nanocomposite membranes. Finally, the performance of prepared nanocomposite membranes was evaluated in both single gas permeation and mixed gas separation experiments.

## 2 Experiment

**2.1 Synthesis and Functionalization of SBA-15 Nanoparticles.** The nanoparticles of SBA-15 was synthesized through the self-assembly of inorganic silica precursor and organic template under hydrothermal conditions. The source of silicon was tetraethylorthosilicate (TEOS) (Merck). The structure-directing agent was cetyltrimethylammonium bromide (CTAB) (Merck). A typical synthesis gel was prepared by adding 5.78 g of TEOS to an aqueous solution containing 1.01 g of CTAB and 0.34 g of NaOH and 30 ml of de-ionized water. After stirring for about 2 h at room temperature, the resulting homogeneous mixture was crystallized under static hydrothermal conditions at 373 K in a homemade Teflon lined autoclave for 72 h. The molar composition of the initial gel mixture was 1.0:0.10:0.30:60 TEOS/CTAB/NaOH/ $H_2O$ . The solid product was obtained by filtration, washed with de-ionized water, dried in vacuum oven at 353 K, and calcined in air at 833 K for 10 h with  $1^\circ C/min$  of heating rate to remove the CTAB. This method results the unmodified version of SBA-15 nanoparticles [25]. We tried two various ways to modify SBA-15: (1) Before removing CTAB, silylation of SBA-15 with dimethylsilane was achieved by immersion of SBA-15 nanoparticles into liquid DMDCS (Merck) for 72 h. Afterwards CTAB was removed by means of Soxhlet extraction apparatus using 250 ml of methanol and 30 ml of aqueous HCL (10 vol %). The extraction process was continued for about 24 h, and then the mixture was filtered and washed with 100 ml of ethanol. In the end, the modified SBA-15 samples were filtered and washed in Soxhlet apparatus with *n*-hexane, and then dried at 333 K in oven [26]. (2) As can be seen in Fig. 1, amine treatment

was performed after silylation of SBA-15 nanoparticles. The silylated mesoporous SBA-15 powder prepared from method (1) were heated at 423 K for 2 h in dry air to remove all adsorbed moisture. The amine solution is prepared by dissolving 0.4 g of 3-aminopropyltrimethoxysilane (APTMS) (Merck) in 100 ml of toluene for 3 h, and then 0.4 g of SBA-15 powder is treated with this preprepared solution in Soxhlet apparatus for 3 h to form covalent bondings with amine in surface of particles. Finally, the excess amines were removed by Soxhlet extraction using methylene chloride ( $CH_2Cl_2$ ) for 5 h and the amine modified SBA-15 particles were dried at room temperature under vacuum.

**2.2 Synthesis of Membranes.** Before using PSF powder in synthesis process, it must be degassed at 423 K for 2 h under vacuum to remove all of its water content. To prepare a sample of SBA-15/PSF nanocomposite membrane, a predetermined amount of the pure PSF was dissolved in *N,N*-dimethylacetamide (DMAC) (Merck) and mixed for 12 h. Then, a corresponding amount of SBA-15 powder was dissolved in *N,N*-dimethylacetamide with a few drops of PSF solution and sonicated in ultrasonic bath for about 20 min. After that, this SBA-15 solution was added to the polymer solution and the mixture was allowed to mix for 4 h at room temperature. Then the mixture was sonicated for 10 min, after which it was allowed to mix for 10 min and this procedure repeated several times to ensure perfect dispersion. The prepared casting solution was cast on a glass substrate using casting blade. The glass substrate was covered with a glass cover to slow down the evaporation rate of the solvent, allowing for the formation of a film with a uniform thickness without curling. After about 1 min, the glass substrate was placed into a coagulation bath of methanol. Solidification of film immediately occurred and the membrane formed and separated from glass substrate. The membrane remained in methanol bath for about 24 h to complete the phase separation process then dried in air at 323 K. Coating solutions were prepared with 1 wt %, 5 wt %, 7 wt %, and 30 wt % of PDMS (Merck) in *n*-hexane. The flat type PDMS/SBA-15/PSF nanocomposite membranes were prepared in a multistep dip-coating procedure: pretreatment with pure *n*-hexane for 4 h, dip coating of the nanocomposite samples with coating solutions for 5 s and then drying at room temperature for 30 min, dip coating of the pretreated supports in coating solutions for 30 s, and then drying at room temperature for overnight and finally completing cross-linking at  $100^\circ C$  for 24 h. At last, a 4 cm diameter circular sample was cut from the film and used for permeation tests. In order to carry out these experiments, two setups were assembled. One is constant pressure apparatus that used for single gas permeation measurements of membranes (Fig. 2). The schematic of membrane module that were used in this apparatus is shown in Fig. 3. The other is multiple gas mixer apparatus that can be used for actual selectivity measurements of membrane. The gas mixer apparatus consisted of a stainless steel cylinder of known volume. The cylinder was connected to vacuum pump and was evacuated before using (Fig. 4).

The first gas cylinder was connected to the apparatus with low pressure and filled the cylinder. Afterward the second gas cylinder

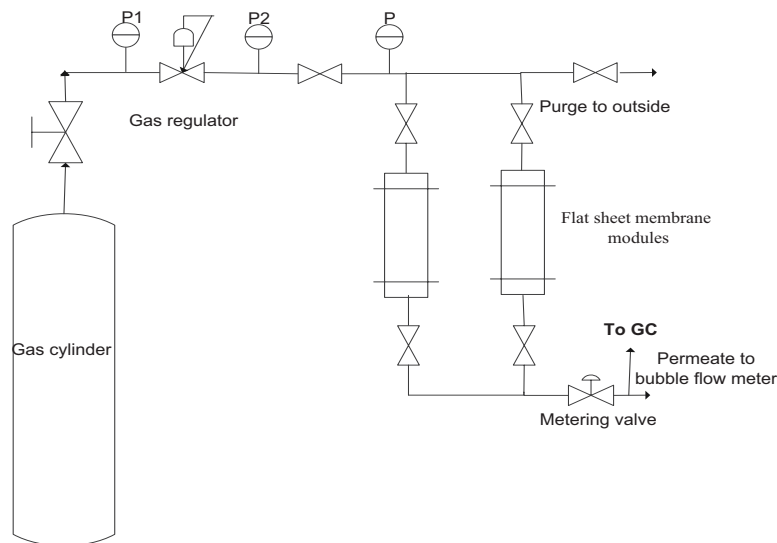


Fig. 2 The single gas permeation experimental setup

was connected to the apparatus too but with higher pressure. Hence, ideally the partial pressures of gases determine the composition of gases in the mixture. For exact determination of compositions of gases in the mixture, the gas chromatography analysis was applied. The composition of permeated gases through the coated SBA-15/PSF membrane is analyzed by gas chromatography method, too. Then selectivities of membranes were measured by gas chromatograph (GC) results. Feed and permeate compo-

sitions were determined by Shimadzo GC-2010 plus GC equipped with a thermal conductivity detector (TCD). The GC column was 2 m long with 1/8 in. inside diameter and packed with TDX-01. The GC temperature profiles were 70°C (oven), 70°C (injector), and 180°C (detector). The samples could be injected into the column and thereby the compositions were measured quickly. Permeate flow rate was measured using a calibrated bubble flow meter (BFM). At steady state condition, gas permeance of species  $i$  was calculated using the following equation:

$$P_i = \frac{22400}{A} \frac{l}{p_2 - p_1} \frac{p_1}{RT} \frac{dV}{dt} \quad (1)$$

where  $A$  is the membrane area ( $\text{cm}^2$ ),  $p_2$  and  $p_1$  are feed or upstream and permeate or downstream pressures (atm), respectively,  $R$  is the universal gas constant ( $6236.56 \text{ cm}^3 \text{ cm Hg/mol K}$ ),  $T$  is the absolute temperature (K),  $dV/dt$  is the volumetric displacement rate of the soap film in the BFM ( $\text{cm}^3/\text{s}$ ), and 22,400 is the number of  $\text{cm}^3$  (STP) of penetrant per mole.

**2.3 Characterization.** Powder XRD) data were recorded using a Philips analytical X-pert diffractometer with  $\text{Cu K}\alpha$  radi-

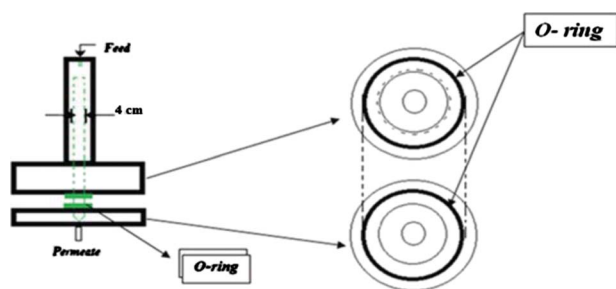


Fig. 3 Schematic view of the dead-end membrane module

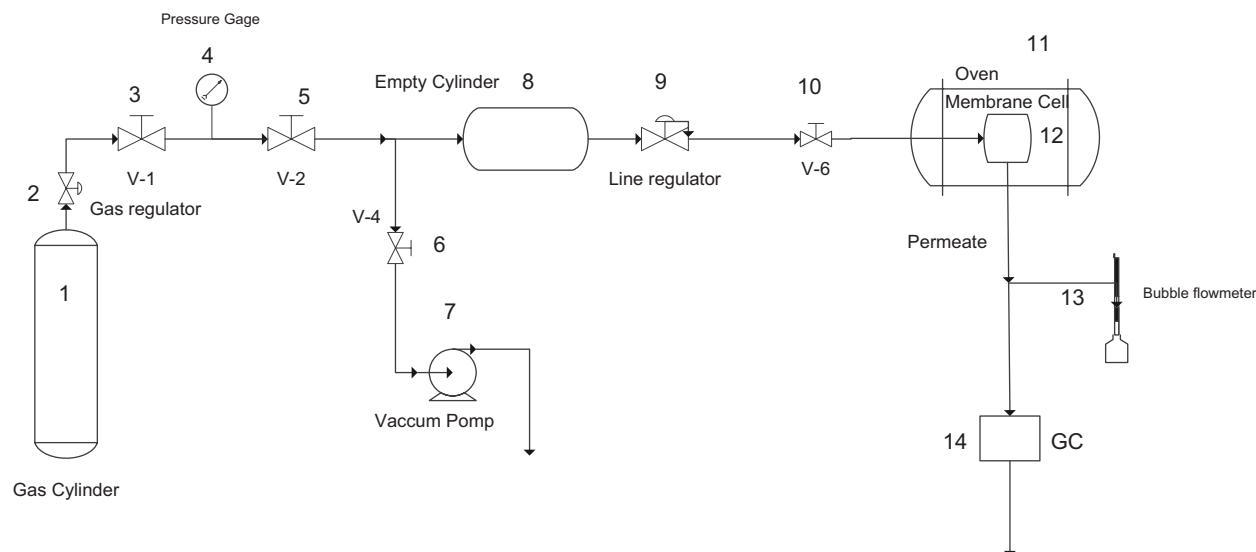


Fig. 4 Experimental setup for mixed gas separation

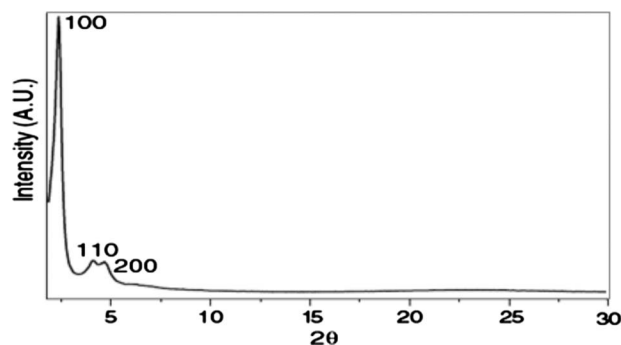


Fig. 5 XRD pattern of SBA-15 particles

tion ( $\lambda = 1.54056 \text{ \AA}$ ) with a step size of  $0.02 \text{ deg/s}$ .  $\text{N}_2$  adsorption isotherms were measured at  $77 \text{ K}$  on a Micromeritics ASAP 2010 analyzer using standard continuous procedures. Samples were first degassed at  $573 \text{ K}$  for  $5 \text{ h}$ . Surface areas and pore size distribution were determined by BET and BJH methods, respectively [27,28]. The particle size analysis for SBA-15 particles was performed by means of Shimadzu sald-2101. SEM (LEO 1450VP) was used to study the morphology of the membranes. The TEMs were obtained on a Zei (LEO912AB) transmission electron microscope device. Thermal stability of membrane was investigated by thermogravimetric analysis (TGA) in Shimadzu (TGA-50/50h) by a heating rate of  $3^\circ\text{C/min}$  up to  $600^\circ\text{C}$ . The permeance tests were carried out in a constant pressure apparatus with micron size bubble flow meters for measuring the volumetric flux of permeated gases. The gases used for permeation measurements were  $\text{CO}_2$ ,  $\text{N}_2$ ,  $\text{O}_2$ , and  $\text{CH}_4$ . Each gas possessed a purity of  $99.99\%$  and was used as received. The feed pressure and temperature kept constant at  $4 \text{ bar}$  and  $298 \text{ K}$ , respectively, for all experiments. Each gas was passed through a membrane five times and the average results were recorded. Permeances were reported in units of GPU. The selectivity of membranes was tested by a gas mixer apparatus that mixes the aforementioned gases based on their partial pressure in the gas mixture. Finally, the composition of permeated gases was investigated by GC analysis.

### 3 Results and Discussion

#### 3.1 Characterization Results of SBA-15 Nanoparticles.

The XRD pattern of the mesoporous material is shown in Fig. 5. The observation of several Bragg peaks at low reflection angles ( $2\theta = 2.5\text{--}7.0$ ), which are relevant to (100), (110), and (210) and can be indexed in a hexagonal lattice and correspond well to the hexagonally arranged pore structure of SBA-15, is the proof of a long-range order and consequently of the good quality of the sample. As the material is not crystalline at the atomic level, no reflections at higher angles are observed.

The particle size analysis result of modified SBA-15 in Fig. 6

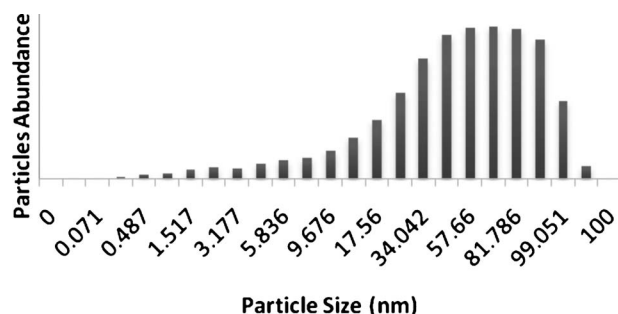


Fig. 6 The particle size distribution of SBA-15 nanoparticles

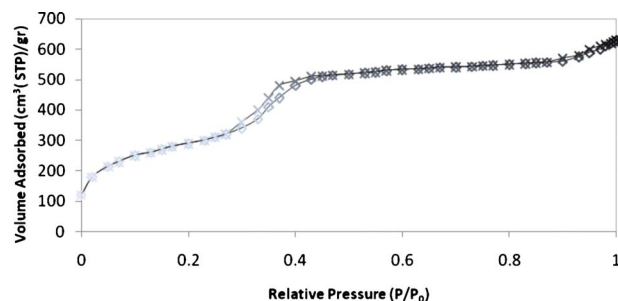


Fig. 7 The  $\text{N}_2$  adsorption-desorption isotherms of SBA-15 particles at  $77 \text{ K}$

shows that the congeries of particles' sizes is mostly between  $40 \text{ nm}$  and  $90 \text{ nm}$  and this proves the nanoscale structure of produced SBA-15 particles.

The nitrogen adsorption-desorption isotherm of extracted SBA-15 at  $77 \text{ K}$  exhibits both a reversible type IV isotherm and a sharp pore filling step at  $p/p_0$   $0.2\text{--}0.3$ , which are characteristic of uniform pores (Fig. 7). The sample shows high specific surface area, approximately  $930 \text{ m}^2/\text{g}$ , and a narrow distribution of pore diameters centered at  $2.1 \text{ nm}$  (Fig. 8), which confirms the XRD analysis results.

The TEM images of the extracted SBA-15 particles in Fig. 9 show the existence of ordered hexagonal structures with particle size in the range  $80 \pm 30 \text{ nm}$ . These XRD patterns, pore size analysis, and TEM results are in agreement with previously published results on nanosized mesoporous silica materials [29,30].

The formation of undesirable gaps or aggregation of inorganic particles in the polymer may happen because of incompatibility between the polymer and the inorganic material, deducting the selectivity and mechanical properties of the membrane. In order to investigate the quality of dispersion of SBA-15 nanoparticles into the polymer matrix, we utilized the SEM images of surface of two kinds of nanocomposite membranes, filled with unmodified

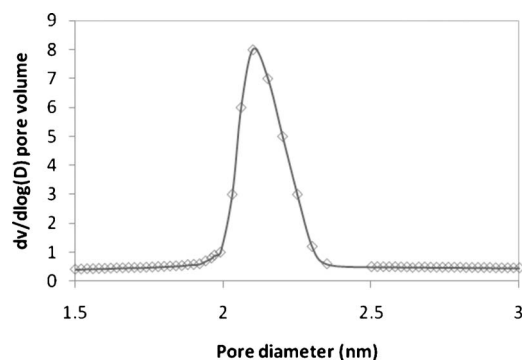


Fig. 8 The pore size distribution of SBA-15 particles

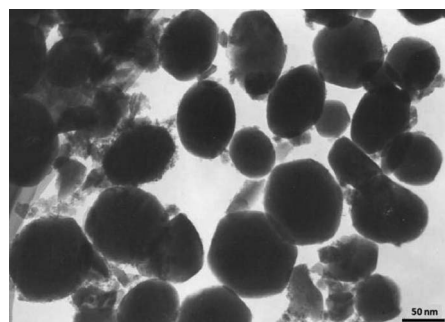


Fig. 9 The TEM image of SBA-15 particles

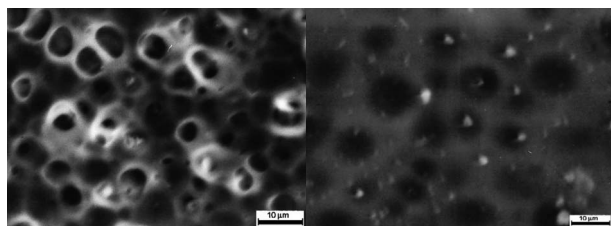


Fig. 10 SEM images of (a) unmodified and (b) DMDCS modified SBA-15/PSF composite membrane

SBA-15 and contained silylated SBA-15. SEM surface images of 20 wt % unmodified and DMDCS modified SBA-15/PSF nanocomposite membranes are shown in Fig. 10. Figure 10(a) shows that in unmodified SBA-15 case in which the unfavorable voids between polymer matrix and inorganic particles present and one can see the agglomeration of particles. However, the dispersion quality of DMDCS modified SBA-15 nanoparticles in polymer matrix appears to be high and there are no distinct voids between two phases. The reason of these two different kinds of behaviors is due to silanol group function. Since they have hydrophilic property and the surface of unmodified SBA-15 nanocomposite membrane is covered by them, the SBA-15 particles easily adhere to each other via hydrogen bonding and form irregular agglomeration in the polymer matrix [31]. However, in modified version, the surface of membrane is silylated with dimethylsilyl groups; hence, the hydrophilic surface of membrane turns to hydrophobic surface. This treatment prevents the particles from being agglomerated and enhances the interaction between particles and polymer producing a composite with well-dispersed mesoporous particles in the polymer matrix.

As can be seen in Fig. 11, TGA results obtained from 3 samples with 0 wt %, 20 wt %, and 40 wt % SBA-15 loading show that the thermal stability of membrane remarkably enhances by increasing the SBA-15 loading in the polymer matrix. The pure PSF membrane has a good thermal stability until 445°C and then loses weight. However, the 20 wt % and 40 wt % SBA-15 loaded membranes have it until 500°C and 560°C, respectively. These results demonstrate that by increasing the loading of thermally stable inorganic SBA-15 into the polymer matrix, the degradation temperature of membrane rises and the thermal stability of membrane significantly improve.

**3.2 Permeance of DMDCS-SBA-15/PSF Nanocomposite Membrane.** The permeance results and ideal selectivity for the neat PSF, unmodified and DMDCS modified SBA-15 and PSF nanocomposite membranes before coating, are shown in Tables 1 and 2, respectively. For all tested gases ( $\text{CO}_2$ ,  $\text{N}_2$ , and  $\text{CH}_4$ ), the enhancement of permeance values is proportional to the amount of SBA-15 loading in the PSF matrix. The addition of 10 wt % and 20 wt % SBA-15 to PSF resulted in at least 70% and 100%

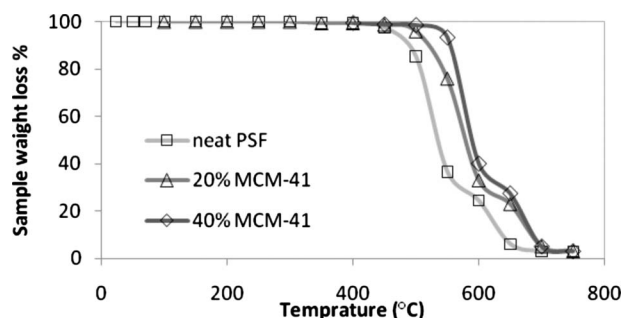


Fig. 11 TGA thermodiagrams of SBA-15/PSF composite membranes with different SBA-15 loading

Table 1 Gas permeance (GPU) ( $\text{GPU}=10^{-6} \text{ cm}^3(\text{STP})/\text{cm}^2 \text{ s cm Hg}$ ) of various gases through the pure polysulfone, unmodified, and DMDCS modified SBA-15 nanocomposite membranes

Membrane	SBA-15 (wt %)	$\text{CO}_2$	$\text{N}_2$	$\text{CH}_4$	$\text{O}_2$
PSF	0	16	0.47	0.45	2.75
U SBA-15/PSF <sup>a</sup>	10	27	0.9	0.93	4.71
DM MCM41/PSF <sup>b</sup>	10	26.7	0.86	0.9	4.62
U SBA-15/PSF	20	32	1.0	1.2	5.35
DM MCM41/PSF	20	31.6	0.99	1.1	5.33
U SBA-15/PSF	40	58	2.6	2.94	10.46
DM MCM41/PSF	40	57.2	2.55	2.91	11

<sup>a</sup>U=unmodified.

<sup>b</sup>DM=DMDCS modified.

increases, respectively, in the permeance of all gases tested. As can be seen, the enhancement of permeance of unmodified version of membrane is obviously decreased the ideal selectivity of pair of gases tested. The reason is probably related to undesirable voids and low dispersion quality of nanoparticles into the in the polymer matrix. The agglomeration of SBA-15 nanoparticles because of hydrophilic nature of them is treated by organosilicon compounds silylation treatment. Organosilicon compounds have many applications in membrane processes, most notably as derivatizing and protecting reagents, intermediates in organic synthesis, and reducing agents. Silicon is considerably less electronegative than either carbon or hydrogen with consequent implications for the polarity of bonds between silicon and other elements. DMDCS is one of the most beneficial kinds of organosilicons for silylation applications. The reason of modification on SBA-15 particles by DMDCS is that the DMDCS introduces a dimethylsilylene group into the substrate molecule and chemically binds thin, water-repellent silica. The surfaces coated by that are neutral, hydrophobic, and nonoily, are not affected by solvents, and are not readily hydrolyzed. The increase in permeance of silylated membrane observed as a function of SBA-15 loading is primarily a consequence of an increase in the diffusivity for each gas. This increase in penetrant diffusivity in modified SBA-15/PSF composite membranes may be attributed to the nonselective microporous voids existing at the SBA-15/polysulfone interface, too. To determine whether the observed increases in permeance were due to the presence of non-selective voids at the SBA-15/PSF interface, the effect of varying the upstream pressure was investigated. For pure PSF,  $\text{N}_2$  permeance is virtually independent of driving pressure, while  $\text{CO}_2$  permeance decreases slightly with increasing upstream pressure. If such nonselective passages exist in the composite membranes, the change in pressure with respect to time on the downstream side of the membrane will be directly proportional to the driving pressure on the upstream side. In the case of a 10% SBA-15/PSF composite membrane, the  $\text{N}_2$  permeance increased slightly from 0.42 GPU (1 bar) to 0.45 GPU (3 bars), and  $\text{CO}_2$  permeance

Table 2 Ideal selectivity for polysulfone, unmodified, and DMDCS modified SBA-15 nanocomposite membranes

Membrane	SBA-15 (wt %)	$\text{O}_2/\text{N}_2$	$\text{CO}_2/\text{CH}_4$
PSF	0	5.4	26
U MCM41/PSF	10	3.2	12.4
DM MCM41/PSF	10	5	22
U SBA-15/PSF	20	2.4	10.6
DM MCM41/PSF	20	5	22
U MCM41/PSF	40	1.4	8.3
DM MCM41/PSF	40	4	14.5

U=unmodified. DM=DMDCS modified.

**Table 3 Gas permeance (GPU) of various gases through the DMDCS modified 20 wt % SBA-15 nanocomposite membranes coated by different concentrations of PDMS solution**

SBA-15 (wt %)	PDMS (wt %)	CO <sub>2</sub>	N <sub>2</sub>	CH <sub>4</sub>	O <sub>2</sub>
20	1	31.6	0.99	1.1	5.33
20	5	30.1	0.97	0.99	5.21
20	7	28.7	0.95	0.96	5.13
20	30	26	0.91	0.93	5.02

decreased slightly from 15 GPU (1 bar) to 14.56 GPU (3 bars). These results demonstrate that the increased permeance observed as a function of SBA-15 loading is not due to the presence of nonselective pores. The increases in permeance at 40 wt % of SBA-15 loading obviously lead to changes in selectivities. However, the selectivities for the composite systems are still much higher than the ideal selectivities, which can still be useful in practical gas separations. The reason of no or slight decrease in selectivity of gases is related to the effect of silylation by DMDCS that prevents SBA-15 particles from being agglomerated and make the gas molecules go through the channels of SBA-15 mesopores instead of bypassing and creation defect shortcuts. The effect of coating of membrane surface by PDMS solution on permeation and ideal selectivity of membrane largely depends on the concentration of coating solution. As shown in Table 3, the per-

**Table 4 Ideal selectivity for DMDCS modified 20 wt % SBA-15 nanocomposite membranes coated by different concentrations of PDMS solution**

MCM41/PSF (wt %)	PDMS (wt %)	O <sub>2</sub> /N <sub>2</sub>	CO <sub>2</sub> /CH <sub>4</sub>
20	1	5	22
20	5	5	22
20	7	5.1	21.9
20	30	7.1	35

**Table 5 Gas permeance (GPU) of various gases in the pure polysulfone, unmodified, DMDCS modified, and APTMS modified SBA-15 nanocomposite membrane**

Membrane	SBA-15 (wt %)	CO <sub>2</sub>	N <sub>2</sub>	CH <sub>4</sub>	O <sub>2</sub>
PSF	0	16	0.47	0.45	2.75
Unmodified MCM41/PSF	20	32	1	1.2	5.35
DMDCS-MCM41/PSF	20	31.6	0.99	1.1	5.33
APTMS-MCM41/PSF	20	29.12	0.80	0.85	4.75

meance of all gases decreases with increasing PDMS solution concentration in 20 wt % SBA-15 nanocomposite membrane. Table 4 demonstrates that membranes coated with low concentrations of PDMS solutions do not change the ideal selectivity of gases. The obtained results reveal that the solution-diffusion mechanism is not the controlling gas transport mechanism in these membranes. This trend can be confirmed by SEM photographs. Figures 12(a)–12(c) show no dense and uniform polymer layers on the porous support surfaces. Contrary to the composite membranes prepared in low concentrations of PDMS solution, ideal selectivities in nanocomposite membrane prepared by 30 wt % PDMS solutions is desirable and in the case of CO<sub>2</sub>/CH<sub>4</sub> it is remarkable. The reason is related to the PDMS properties. PDMS has weak molecular sieve ability due to its weak intermolecular forces, resulting in broad distribution of intersegmental gap sizes responsible for gas diffusion. Despite the slight reduction in permeabilities of modified membranes after coating is caused by reducing diffusivity of membranes. This process makes O<sub>2</sub>/N<sub>2</sub> and especially CO<sub>2</sub>/CH<sub>4</sub> ideal selectivities enhances even more than those before coating by PDMS solution compared with neat polymeric membrane.

**3.3 Permeance of APTMS–SBA-15/PSF Nanocomposite Membrane.** The APTMS treatment of mesoporous SBA-15 before introducing it into the polymer matrix was performed to increase the CO<sub>2</sub> adsorption capacity of membrane. As can be seen in Table 5, the enhancement in permeance of all versions of 20

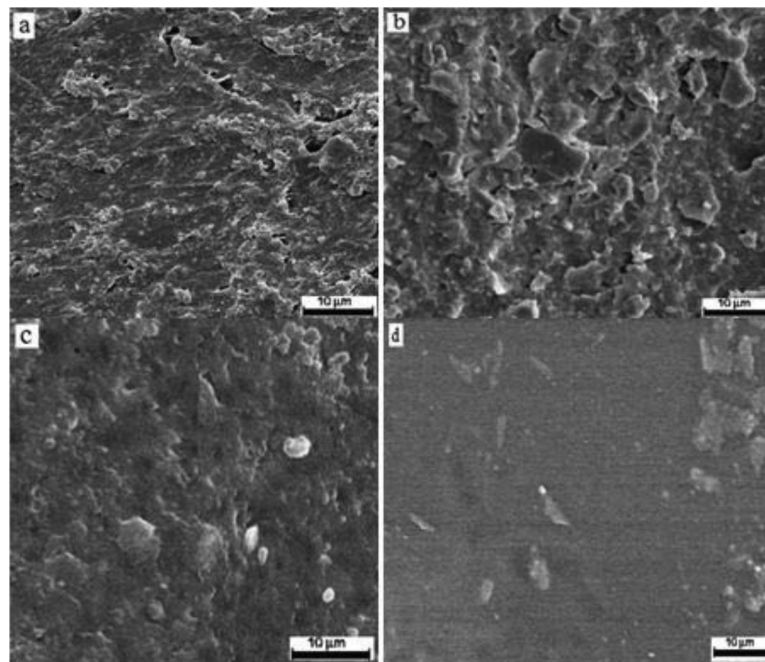


**Fig. 12 SEM photographs of the surface of SBA-15/PSF composite membranes coated with different PDMS solution concentrations: (a) 1 wt %, (b) 5 wt %, (c) 7 wt %, and (d) 30 wt %**

**Table 6 Ideal selectivity for polysulfone, unmodified, DMDCS modified, and APTMS modified SBA-15 nanocomposite membrane**

Membrane	SBA-15 (wt %)	O <sub>2</sub> /N <sub>2</sub>	CO <sub>2</sub> /CH <sub>4</sub>
PSF	0	5.4	26
Unmodified MCM41/PSF	20	2.4	10.6
DMDCS-MCM41/PSF	20	5	22
APTMS-MCM41/PSF	20	5	28

wt % SBA-15/PSF nanocomposite membranes before coating is obvious and that is because of introduction of SBA-15 nanoparticles into the polymer matrix. The only distinct difference is the ideal selectivities (Table 6). The enhancement of CO<sub>2</sub>/CH<sub>4</sub> selectivity of APTMS modified membrane is much more than those of unmodified and DMDCS modified membranes. It is probably related to amine capability of CO<sub>2</sub> extra sorption. It has been reported that CO<sub>2</sub> adsorption in amine modified mesoporous SBA-15 can be enhanced via formation of surface carbamate groups [26]. Another role of APTMS as a “sticker” is conducted by its aminopropyl groups, attracting and anchoring the SBA-15 particles tightly adhered to PSF polymer by increasing van der Waals force [32,33]. The low concentration PDMS solution did not have significant influence on gas permeance of membranes. However, the 30 wt % PDMS solution increased ideal selectivity and also decreased permeance of membranes as expected (Table 7 and 8). The net result of coating is improvement in permeances and also ideal selectivities of membranes compared with neat polymeric membrane. The additional enhancement of CO<sub>2</sub>/CH<sub>4</sub> ideal selectivity of membranes from 28 to 38.2 is another novelty that was achieved by the PDMS surface coating of membranes. The comparison between this work and previous researches is

**Table 7 Gas permeance (GPU) of various gases in the DMDCS and APTMS modified 20wt % SBA-15 nanocomposite membranes coated by 30 wt % PDMS solution**

Membrane	SBA-15 (wt %)	PDMS (wt %)	CO <sub>2</sub>	N <sub>2</sub>	CH <sub>4</sub>	O <sub>2</sub>
DMDCS-MCM41/PSF	20	30	26	0.91	0.93	5.02
APTMS-MCM41/PSF	20	30	23	0.52	0.52	4.04

**Table 8 Ideal selectivity for DMDCS and APTMS modified 20 wt % SBA-15 nanocomposite membranes coated by 30 wt % PDMS solution**

Membrane	SBA-15 (wt %)	PDMS (wt %)	O <sub>2</sub> /N <sub>2</sub>	CO <sub>2</sub> /CH <sub>4</sub>
DMDCS-MCM41/PSF	20	30	7.1	35
APTMS-MCM41/PSF	20	30	7.2	38.2

**Table 9 Ideal selectivity comparison of 20 wt % SBA-15/PSF nanocomposite membranes of this work with previous researches**

Nanocomposite membrane	Modifier agent	Ideal selectivity CO <sub>2</sub> /CH <sub>4</sub>	Ideal selectivity O <sub>2</sub> /N <sub>2</sub>	References
20 wt % MCM-41/PSF	No modifier	18.9	5.47	[16]
20 wt % modified MCM-41/PSF	Trimethylchlorosilane (TMCS)	23	5	[18]
20 wt % modified MCM-41/PSF	Aminopropyltriethoxysilane (APTES)	28	5	[18]
20 wt % modified SBA-15/PSF coated by PDMS	Dimethyldichlorosilane (DMDCS)	35	7.1	Present work
20 wt % modified SBA-15/PSF coated by PDMS	Aminopropyltrimethoxysilane (APTMS)	38.2	7.2	Present work

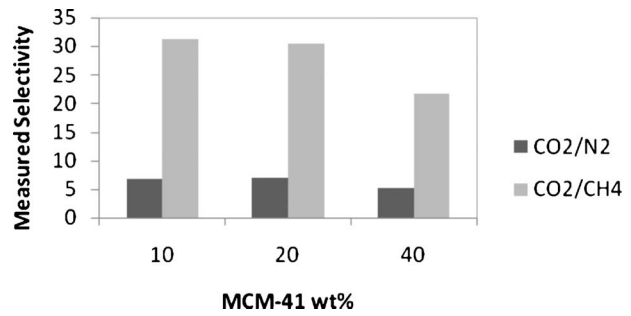


**Fig. 13 Measured selectivities for 30 wt % PDMS coated DMDCS modified membranes with different loadings of SBA-15 in PSF matrix at 4 bars and 298 K using 50-50 vol % O<sub>2</sub>-N<sub>2</sub> and CO<sub>2</sub>-CH<sub>4</sub> gas mixtures, respectively**

available in Table 9 [16–18]. Table 9 compares the ideal selectivities of CO<sub>2</sub>/CH<sub>4</sub> and O<sub>2</sub>/N<sub>2</sub> for PDMS coated DMDCS and APTMS 20 wt % SBA-15/PSF membrane that is fabricated in this study with TMCS and APTES 20 wt % SBA-15/PSF and unmodified 20 wt % SBA-15/PSF that synthesized by other previous researchers. As can be seen in Table 9, the synthesized membranes in this work have superior selectivity for both CO<sub>2</sub>/CH<sub>4</sub> and O<sub>2</sub>/N<sub>2</sub> compared with the other researches. The reasons are probably attributed to surface modification of inorganic phase and proper coating quality of surface prepared nanocomposite membrane by PDMS, which is suitable for membrane coating applications.

**3.4 Actual Selectivity Measurements.** Figures 13 and 14 represent the measured selectivities for 30 wt % PDMS coated DMDCS and APTMS modified membranes with different loading of SBA-15 in PSF matrix at 4 bars and 298 K using a gas mixture containing 50-50 vol % of O<sub>2</sub>, N<sub>2</sub>, CO<sub>2</sub>, and CH<sub>4</sub>, respectively. The selectivity of gases is calculated by Eq. (2):

$$\alpha_{AB} = \frac{y_A/y_B}{x_A/x_B} \quad (2)$$

where  $x_A$  and  $y_A$  are the mole fractions of species A and  $x_B$  and  $y_B$  are the mole fractions of species B in the feed and permeate streams. As shown in Figs. 13 and 14, the selectivity of all DMDCS and also APTMS modified membranes coated by 30 wt % PDMS is higher than ideal selectivities of uncoated membranes due to the good coating quality of surface and treating the possible surface defects of membrane with selective PDMS. PDMS coating of membranes makes solubility of gases like CO<sub>2</sub> and O<sub>2</sub> increase more than CH<sub>4</sub> and N<sub>2</sub> and this enhances the CO<sub>2</sub>/CH<sub>4</sub> and O<sub>2</sub>/N<sub>2</sub> selectivities of SBA-15 nanocomposite membranes. As can be seen in Figs. 15 and 16, in both DMDCS and APTMS modified versions of 30 wt % PDMS coated and 20 wt % SBA-15/PSF membrane, permeances of all gases tested reduced compare with uncoated nanocomposite membranes but still much

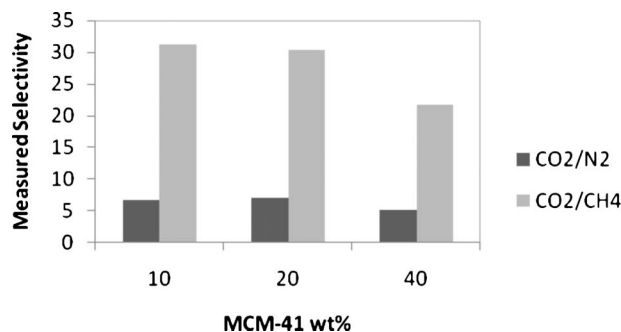


**Fig. 14 Measured selectivities for 30 wt % PDMS coated APTMS modified membranes with different loadings of SBA-15 in PSF matrix at 4 bars and 298 K using 50-50 vol % O<sub>2</sub>-N<sub>2</sub> and CO<sub>2</sub>-CH<sub>4</sub> gas mixtures, respectively**

higher than neat PSF membrane. The reason of reduction in permeances is related to a reduction in diffusivity of gases in uncoated membranes by coating the surface of membrane and increasing the resistant against diffused molecules through SBA-15 pores. The net result is by PDMS coating of APTMS modified SBA-15/PSF nanocomposite membranes, despite the reduction in permeances of all gases tested compared with uncoated membranes, the permeances and selectivities of all tested gases is much higher than neat PSF membrane. In addition, the enhancement in selectivity of CO<sub>2</sub>/CH<sub>4</sub> is remarkable and that is because of using APTMS for additional adsorption of CO<sub>2</sub>.

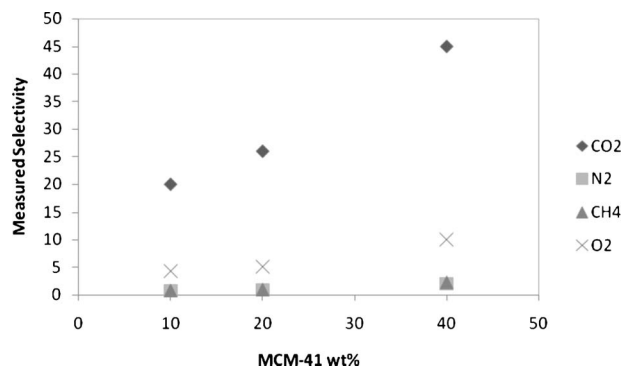


**Fig. 15 Measured permeances (GPU) for 30 wt % PDMS coated DMDCS modified membranes with different loadings of SBA-15 in PSF matrix at 4 bars and 298 K using a mixture that contained 25 vol % of each gas**

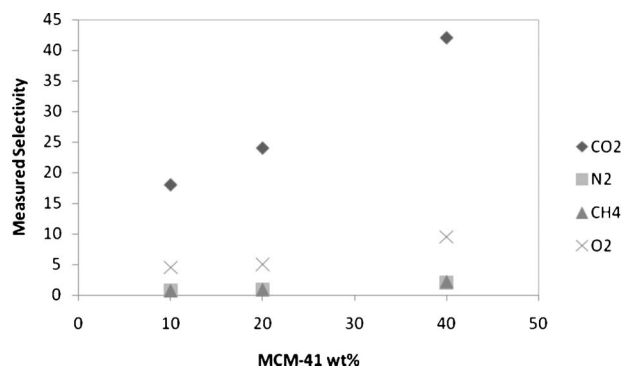


**Fig. 16 Measured permeances (GPU) for 30 wt % PDMS coated APTMS modified membranes with different loadings of SBA-15 in PSF matrix at 4 bars and 298 K using a mixture that contained 25 vol % of each gas**

## 4 Conclusion

Mesoporous SBA-15 offers the favorable effect of dramatically increasing the permeance of the composite over that of PSF. However, without silylation of SBA-15 particles, the enhancement in permeance causes reduction in selectivities of gases. The silylation by DMDCS makes trimethylsilyl groups, which after modification, decorate the internal surface of SBA-15, and prevent the unnecessary functionality for hydrogen bonding, which results in better dispersion quality and so permeance enhancement without losing selectivity. An addition functionalization by APTMS makes the CO<sub>2</sub>/CH<sub>4</sub> selectivity dramatically rises even more than those modified by DMDCS, while the 21 Å pore size is large enough to readily enable penetration of the polymer. Together, these attributes make SBA-15 an attractive additive for universally enhancing the gas permeance of PSF without sacrificing its selectivity. This enhancement in permeance is likely attributable to a reduced resistance to gas flow inside the large channels of SBA-15. The performance of PDMS coated membranes were investigated, SEM photographs showed that the PDMS layer on the composite membranes prepared in low concentrations was not uniform, and PDMS solution penetrated into pores of supports. Experimental results clearly indicated that the undesirable penetration during the dip-coating stage could be avoided by increasing the concentration of PDMS coating solution. The coated membranes by 30 wt % PDMS solution showed remarkable enhancement in selectivities of all gases tested with slight decreasing in permeances of them. The reasons are related to high quality coating of surface of membranes and also the thickness of coated film because of high concentration of coating solution. In summary, introducing SBA-15 nanoparticles into the matrix of polymer and surface coating of these membranes result in both higher permeance and selectivity for gas separation compared with neat polymeric membranes.

## References

- [1] Robeson, L. M., 1991, "Correlation of Separation Factor Versus Permeance for Polymeric Membranes," *J. Membr. Sci.*, **62**, pp. 165–185.
- [2] Merkel, T. C., Freeman, B. D., Spontak, R. J., He, Z., Pinnau, I., Meakin, P., and Hill, A. J., 2002, "Ultrapervaporation, Reverse-Selective Nanocomposite Membranes," *Science*, **296**, pp. 519–522.
- [3] Boom, J. P., Punt, I. G. M., Zwijnenberg, H., de Boer, R., Bargeman, D., Smolders, C. A., and Strathmann, H., 1998, "Transport Through Zeolite Filled Polymeric Membranes," *J. Membr. Sci.*, **138**, pp. 237–258.
- [4] Kresge, C. T., Leonowicz, M. E., Roth, W. J., Vartulli, J. C., and Beck, J. S., 1992, "Ordered Mesoporous Molecular Sieves Synthesized by a Liquid-Crystal Template Mechanism," *Nature (London)*, **359**, pp. 710–712.
- [5] Beck, J. S., Vartulli, J. C., Roth, W. J., Leonowicz, M. E., Kresge, C. T., Schmitt, K. D., Chu, C. T. W., Olson, D. H., Sheppard, E. W., McCullen, S. B., Higgins, J. B., and Schlenker, J. L., 1992, "A New Family of Mesoporous Molecular Sieves Prepared With Liquid Crystal Templates," *J. Am. Chem. Soc.*, **114**, pp. 10834–10843.
- [6] Moermans, B., Beuckelaer, W. D., Vankelcomm, I. F. J., Ravishanker, R., Martens, J. A., and Jacobs, P. A., "Incorporation of Nano-Sized Zeolites in Membranes," *Chem. Commun. (Cambridge)* **2000**, pp. 2467–2468.
- [7] Wang, Y. C., Fan, S. C., Lee, K. R., Li, C. L., Huang, S. H., Tsai, H. A., and Lai, J. Y., 2004, "Polyamide/SDS-Clay Hybrid Nanocomposite Membrane Application to Water-Ethanol Mixture Pervaporation Separation," *J. Membr. Sci.*, **239**, pp. 219–226.
- [8] Yeh, J. M., Yu, M. Y., and Liou, S. J., 2003, "Dehydration of Water-Alcohol Mixtures by Vapor Permeation Through PVA/Clay Nanocomposite Membrane," *J. Appl. Polym. Sci.*, **89**, pp. 3632–3638.
- [9] Gao, Z., Yue, Y., and Li, W., 1996, "Application of Zeolite-Filled Pervaporation Membrane," *Zeolites*, **16**, pp. 70–74.
- [10] Zimmerman, C. M., Singh, A., and Koros, W. J., 1997, "Tailoring Mixed Matrix Composite Membranes for Gas Separations," *J. Membr. Sci.*, **137**, pp. 145–154.
- [11] Mahajan, R., and Koros, W. J., 2000, "Factors Controlling Successful Formation of Mixed Matrix Gas Separation Materials," *Ind. Eng. Chem. Res.*, **39**, pp. 2692–2696.
- [12] Gür, T. M., 1994, "Permeability of Zeolite Filled Polysulfone Gas Separation Membranes," *J. Membr. Sci.*, **93**, pp. 283–289.
- [13] Okumus, E., Gurkan, T., and Yilmaz, L., 1994, "Development of a Mixed-Matrix Membrane for Pervaporation," *Sep. Sci. Technol.*, **29**, pp. 2451–2473.
- [14] Vu, D. Q., Koros, W. J., and Miller, S. J., 2003, "Mixed Matrix Membranes Using Carbon Molecular Sieves. I. Preparation and Experimental Results," *J. Membr. Sci.*, **211**, pp. 311–334.
- [15] Wang, H. T., Holmberg, B. A., and Yan, Y. S., 2002, "Homogeneous Polymer-

- Zeolite Nanocomposite Membranes by Incorporating Dispersible Template-Removed Zeolite Nanocrystals," *J. Mater. Chem.*, **12**, pp. 3640–3643.
- [16] Reid, B. D., Ruiz-Trevino, F. A., Musselman, I. H., Kenneth, J., Balkus, J., and Ferraris, J. P., 2001, "Gas Permeance Properties of Polysulfone Membranes Containing the Mesoporous Molecular Sieve SBA-15," *Chem. Mater.*, **13**, pp. 2366–2373.
- [17] Kim, S., Marand, E., Ida, J., and Gulians, V. V., 2006, "Polysulfone and Mesoporous Molecular Sieve MCM-48 Mixed Matrix Membranes for Gas Separation," *Chem. Mater.*, **18**, pp. 1149–1155.
- [18] Kim, S., and Marand, E., 2008, "High Permeability Nano-Composite Membranes Based on Mesoporous MCM-41 Nanoparticles in a Polysulfone Matrix," *Microporous Mesoporous Mater.*, **114**, pp. 129–136.
- [19] Shimizu, S., Matsuyama, H., and Teramoto, M., 2005, "Gas Separation Properties of Polyimide Membrane Containing Mesoporous Material," *ICOM 2005*, Seoul, South Korea, Aug., Vol. 177, pp. 21–26.
- [20] Ladewig, B., Martin, D., Knott, R., Diniz da Costa, J. C., and Lu, G. Q., 2007, "Nafion-MPMDMS Nanocomposite Membranes With Low Methanol Permeability," *Electrochem. Commun.*, **9**, pp. 781–786.
- [21] Stern, S. A., Shah, V. M., and Hardy, B. J., 1987, "Structure-Permeance Relationships in Silicone Polymers," *J. Polym. Sci., Part B: Polym. Phys.*, **25**, pp. 1263–1298.
- [22] Shah, V. M., Hardy, B. J., and Stern, S. A., 1986, "Solubility of Carbon Dioxide, Methane, and Propane in Silicone Polymers: Effect of Polymer Side Chains," *J. Polym. Sci., Part B: Polym. Phys.*, **24**, pp. 2033–2047.
- [23] Fleming, G. K., and Koros, W. J., 1986, "Dilation of Polymers by Sorption of Carbon Dioxide at Elevated Pressures. I. Silicone Rubber and Unconditioned Polycarbonate," *Macromolecules*, **19**, pp. 2285–2291.
- [24] Merkel, T. C., Bondar, V. I., Nagai, K., Freeman, B. D., and Pinnau, I., 2000, "Gas Sorption, Diffusion, and Permeation in Poly(Dimethylsiloxane)," *J. Polym. Sci., Part B: Polym. Phys.*, **38**, pp. 415–434.
- [25] Merkel, T. C., Gupta, R. P., Turk, B. S., and Freeman, B. D., 2001, "Mixed-Gas Permeation of Syngas Components in Poly(Dimethylsiloxane) and Poly(1-Trimethylsilyl-1-Propyne) at Elevated Temperatures," *J. Membr. Sci.*, **191**, pp. 85–94.
- [26] Chen, H., and Wang, Y., 2002, "Preparation of SBA-15 With High Thermal Stability and Complementary Textural Porosity," *Ceram. Int.*, **28**, pp. 541–547.
- [27] Kim, S., Ida, J., Gulians, V. V., and Lin, Y. S., 2005, "Tailoring Surface Properties of MCM-48 Silica by Bonding 3-Aminopropyltriethoxysilane for Selective Adsorption of Carbon Dioxide," *J. Phys. Chem. B*, **109**, pp. 6287–6293.
- [28] Brunauer, S., Emmett, P. H., and Teller, E., 1938, "Adsorption of Gases in Multimolecular Layers," *J. Am. Chem. Soc.*, **60**, pp. 309–319.
- [29] Constantinescu, F., and Blum, J., 1995, "Adsorption Characterisation of the Dealumination Effect on H-Mordenites," *J. Porous Mater.*, **2**, pp. 35–41.
- [30] Cai, Q., Luo, Z. S., Pang, W. Q., Fan, Y. W., Chen, X. H., and Cui, F. Z., 2001, "A Simple Route for Preparing Radiolarian-like Mesoporous Silica from Water-Diethyl Ether Binary Solvent System," *Chem. Mater.*, **13**, pp. 258–263.
- [31] Oleg, Yu. P., Telbiz, G. M., and Rossokhaty, V. K., 2006, "Effect of Solvent Nature on Liquid-Phase Self-Assembly of MEH-PPV/SBA-15 Guest-Host Composites," *J. Mater. Chem.*, **16**, pp. 2485–2489.
- [32] Sun, Y., Zhang, Z., and Wong, C. P., 2005, "Study on Mono-Dispersed Nano-Size Silica by Surface Modification for Underfill Applications," *J. Colloid Interface Sci.*, **292**, pp. 436–444.
- [33] Nishiyama, N., Park, D. H., Koide, A., Egashira, Y., and Ueyama, K., 2001, "Enhancement of Hydrothermal Stability and Hydrophobicity of a Silica MCM-48 Membrane by Silylation," *J. Membr. Sci.*, **182**, pp. 235–244.